

PREDICTION OF ELECTRON FLUXES IN A CIRCULAR POLAR ORBIT: SELECTION OF PREDICTORS

A.O. Belova

*Lomonosov Moscow State University,
Moscow, Russia, belova.ao20@physics.msu.ru*

I.N. Myagkova

*Lomonosov Moscow State University,
Skobel'syn Institute of Nuclear Physics,
Moscow, Russia, irina@srd.sinp.msu.ru*

Abstract. We have investigated the relationship of variations in >0.7 and >2 MeV electron fluxes of Earth's outer radiation belt in a circular polar orbit with solar wind and interplanetary magnetic field parameters, as well as with geomagnetic indices and the logarithmic electron flux in the geostationary orbit in order to explore the possibility of predicting them. We have selected the optimal input features for predicting electron fluxes in low polar orbits, which is important for ensuring the radiation safety of future space missions.

We have examined integral and maximum electron

fluxes of these energies over the span of a day. We have obtained forecasts with a horizon of 1 and 2 days for an interval of 2 months in 2020 for daily maximum and integral fluxes based on linear regression.

Keywords: Earth's radiation belts, relativistic electron fluxes, forecasting, machine learning, circular polar orbit.

INTRODUCTION

Radiation conditions in near-Earth space are largely determined by charged particle fluxes in Earth's radiation belts (ERB). The contribution of ERB particles is especially significant during solar minimum when there are practically no solar cosmic ray fluxes. While particle fluxes of inner ERB are relatively stable and there are generally accepted models that can be used to reliably predict particle fluxes in it, Earth's outer radiation belt (EORB) is very unstable: its electron fluxes can vary by several orders of magnitude within 24 hours. EORB electrons were first detected a long time ago — during the second space flight in the history of mankind, using scientific equipment of SINP MSU [Vernov et al., 1958]. Since then, a large number of experiments on recording EORB electrons by Russian and foreign spacecraft (SC) have been carried out [Williams et al., 1968; Li et al., 2001; Kataoka, Miyoshi, 2008; Kuznetsov et al., 2007; Li, Hudson, 2019; Osedlo et al., 2022; Stepanova et al., 2024]. Nonetheless, the problem of reliably predicting the state of EORB through modeling has not yet been solved. This is due to the fact that to date there is no generally accepted theory of acceleration and scattering of EORB electrons which could explain the available set of experimental data.

Monitoring and prediction of EORB electrons is also of practical interest since the influence of high fluxes of relativistic and sub-relativistic EORB electrons can negatively affect the electronic equipment installed on board SC because Single Event Upsets (SEU), both reversible and irreversible, can occur when the electrons penetrate into integrated circuits [Cole, 2003; Belov et al., 2004; Romanova et al., 2005; Iucci et al., 2005; Pilipenko et al., 2006; Kudela, 2013] (in English literature, they are also called killer electrons), SC can be electrified as well [Novikov, Voronina, 2021].

On the one hand, it is impossible to predict with sufficient accuracy variations in EORB electron fluxes through theoretical calculations; on the other hand, there is a practical need to predict them to ensure radiation safety with modern machine learning methods that help identify the relationships between analyzed variables by approximating empirical dependences.

Satellite measurements made in Earth's inner magnetosphere are employed not only to describe the EORB dynamics, but also to develop forecasting models based on machine learning. Data from GOES satellites having a long time series of experimental measurements is most often applied for these purposes because GOES SC have been launched since the 1970s (see, e.g., [Wei et al., 2018; Myagkova et al., 2019; Sun et al., 2021; Landis et al., 2022; Son et al., 2022]). Currently, one of the most widely used methods for predicting the total relativistic electron flux over the span of a day (fluence) in EORB is the forecast presented on the portal of the Space Weather Prediction Center [<http://www.swpc.noaa.gov/>]. This model, known as REFM (Relativistic Electron Forecast Model), was developed based on research evidence [Baker et al., 1990]. The forecast uses the fact that daily fluences of >2 MeV electrons, measured in geostationary orbit, can be predicted a day ahead with the aid of a linear filter, which utilizes the SW velocity or the geomagnetic indices K_p and AE as input data. Studies have shown the presence of characteristic temporal dynamics in the behavior of electron fluxes in geostationary orbit. A significant increase in the electron flux is observed two days after the SW velocity reaches its maximum and three days after recording peak values of the geomagnetic indices. This time delay is due to the structural features of SW streams, including the region of the increased interplanetary magnetic

field (IMF) preceding the SW velocity peak. The IMF peak initiates geomagnetic activity leading to an increase in K_p . Thus, there is a significant delay between the geomagnetic indices (K_p , AE) and an increase in the electron flux as compared to direct measurements of SW parameters. It is worth mentioning the model for predicting >2 MeV relativistic electron fluxes in geostationary orbit, which is based on solving a system of continuity equations, provided that particle acceleration is affected not only by the SW velocity, but also by geomagnetic activity, and losses are influenced by the SW density. Taking into account additional factors having an effect on electron acceleration and losses in ERB made it possible to improve the accuracy and stability of forecasts [Lyatsky, Khazanov, 2008]. For low energies (1 eV – 40 keV), there is also a forecasting model with a 1-hr horizon based on IMF and SW velocity [Denton et al., 2016]. In addition to solving the continuity equations, there are other methods for predicting electron fluxes. For example, Potapov et al. [2016] employed the multiple regression method with a sliding window to predict the $>1\div 2$ MeV relativistic electron flux. Particularly noteworthy is the NARMAX model (nonlinear autoregression with running mean with external input signals) [Balikhin et al., 2011]. One of the stages of the algorithm involves analyzing the Error Reduction Ratio ERR , which makes it possible to rank the parameters affecting fluxes in ERB. It was this analysis that led the authors to the conclusion that the SW density, rather than its velocity, has the greatest effect on electron fluxes in ERB. Given a fixed density, the fluxes increase as the velocity reaches a certain saturation level decreasing with increasing SW density. There is also an approach to predicting charged particle fluxes in ERB by the BAS Global Dynamic Radiation Belt Model [Glauert et al., 2014], based on solving the 3D Fokker-Planck equation. The developed model relies on a comprehensive approach to describing the dynamics of charged particles and includes the following physical processes: radial diffusion of particles in Earth's magnetosphere, particle—wave interaction, and collisional processes responsible for particle losses from radiation belts.

A separate problem is to predict fluxes of relativistic and sub-relativistic electrons detected in circular polar orbits, where the satellite crosses EORB four times during one orbital period — twice in the Southern Hemisphere and twice in the Northern Hemisphere. For circular polar orbits, we can solve the problem of predicting the daily maximum electron flux and/or the total flux (fluence), which is accumulated over the span of a day at all satellite crossings of EORB.

This study focuses on EORB and variations in electron fluxes in the circular polar orbit similar to the orbit considered in [Botek et al., 2023]. The authors have predicted electron fluxes with energies 500–600 keV and 1–2.4 MeV for the circular polar orbit, using data from PROBA-V SC and the long short-term memory (LSTM) model, for which data on the satellite's position and the geomagnetic index SYM was taken as input parameters. An array of measurements for 2015–2018 was used as initial da-

ta. For EORB, the Root Mean Square Error (RMSE) was 0.153 for 500–600 keV with a horizon of 1 day.

The relevance of this study stems from the fact that a similar low polar orbit is planned to be employed in the Russian Orbital Station (ROS) project. In this regard, the development of methods for predicting radiation conditions at such orbits is of considerable practical interest for ensuring the safety of SC and crews.

The purpose of this study is to develop methods for predicting variations in >0.7 and >2 MeV EORB relativistic and sub-relativistic electron fluxes in the circular polar orbit, utilizing SW, IMF parameters, geomagnetic indices, and electron flux in geostationary orbit as input features, as well as to assess the effectiveness of such forecasting.

1. FORECASTING METHOD

Spacecraft data processing, machine learning model training, and forecasting have been carried out with a program developed using Python.

In this paper, we address the problem of predicting time series, where the target variable is y_{t+h} , with h being the forecast horizon (the number of days for which the forecast is made), and features are formed based on the lags (delays) of the series:

$$X_t = \{y_{t-1}, y_{t-2}, \dots, y_{t-p}, F_{t-1}, F_{t-2}, \dots, F_{t-p}\},$$

where F_t is a time series of additional features, such as SW parameters, etc., and p is the number of lags. The prediction formula in the general form is

$$y_{t+h} = f(X_t),$$

where f is a prediction function.

We have employed a machine learning model (linear regression) to predict electron fluxes in the circular polar orbit. Linear regression is a regression model used in statistics for the dependence of one (explicable) variable \vec{y} on another or several other variables \vec{X} with a linear dependence function.

$$y_i = a_1 X_{1i} + a_2 X_{2i} + \dots + a_m X_{mi} + a_0,$$

where i is the observation number; a_0, a_1, \dots, a_m are the parameters to be estimated (for more detail, see [Demidenko, 1981]).

In order to compare the quality of forecasts, made using linear regression in the future, we produced a forecast with a naive model. The naive forecasting model is a model whose value at a forecast point is equal to the last known value of the predicted variable.

2. INPUT DATA

We have selected the following features as input data for forecasting.

1. SW parameters at the Lagrange point L1 between Earth and the Sun: SW velocity and density obtained by SWEPAM (Solar Wind Electron Proton Alpha Monitor) during the experiment on ACE SC.

2. IMF parameters: the field vector magnitude B_t and B_z obtained by the ACE MAG magnetometer.

3. Geomagnetic indices: Dst and K_p from the World Data Center for Geomagnetism (Kyoto).

4. Logarithm of maximum and integral electron fluxes over the span of a day in EORB (>0.8 , >2 MeV) from GOES measurement data.

We have used three-hour K_p , hourly Dst , and other features averaged over 1 min. The maximum flux was defined as the largest 1-min average for each parameter for each specific day.

The data was acquired from open sources, namely from the SINP MSU Space Weather Data Analysis Center [<https://swx.sinp.msu.ru/>].

Data from the first three stations was converted to daily values by calculating the mean and the maximum magnitude per day. After such conversions, the number of features doubled. Later, we analyzed the significance of each of these features, and left only one of two similar variants for each of them.

The choice of the first three stations is based on the experience of forecasting the daily average flux in geostationary orbit in [Koons, Gorney, 1991; Ling et al., 2010], as well as in recent works by the SINP MSU research team [Myagkova et al., 2021; Kalegaev et al., 2019, 2023].

Time series forecasting models are usually trained on the τ previous values of the series. τ is called the window width. We have adopted a window width of a multidimensional time series equal to 26 days. Lags equal to 1 (only for the forecast for 1 day in advance), 2, 3, 4, 5, 6, 7, 13, and 26 days were taken from this window. The lags corresponding to one week are applied to the model to effectively use the current available information about the features; the lags equal to 13 and 26 days are linked to the 25–27 day solar rotation period. As shown below, the recurrent fluxes associated with solar rotation can have a significant effect on IMF and SW parameters, thereby considerably altering charged particle fluxes in radiation belts.

Our work relies on a 9-month data array from June 1, 2019 to March 1, 2020, which was divided into training

and test datasets as 7:2. The data from June 01, 2019 to December 31, 2019 inclusive was used for the training dataset. The data from January 01, 2020 to March 01, 2020 was utilized as the test dataset — independent data employed to assess the forecast quality.

In the study, we selected a limited time interval corresponding to the period of minimum geomagnetic activity. This approach provided the most stable conditions for conducting a comparative analysis whose main purpose was to compare the temporal dynamics of daily integral and maximum electron fluxes in EORB at low altitudes with the similar dynamics of electron fluxes recorded in geostationary orbit.

This study was carried out taking into account the fact that forecasting models of electron fluxes in geostationary orbit based on machine learning methods have been developed and successfully operate.

The training was done on the basis of data on EORB electron fluxes, measured by Meteor-M2 (launched on July 08, 2014). The forecast was made for daily maximum and integral electron fluxes in EORB (>0.7 , >2 MeV). The Meteor-M2 orbit is circular and sun-synchronous, with an altitude at the ascending node $h=832$ km, an inclination $i\approx 98.85^\circ$, and an orbital period $T=101.3$ min. Thus, during one orbital period the satellite crossed EORB four times (Figure 1).

From the data collected during each orbital period, we identified intervals where the McIlwain parameter L varied from 3 to 6. Integral fluxes were calculated for these intervals, using the trapezoid formula; the daily integral flux was obtained by summing integral fluxes for each such interval. The daily maximum flux was computed as the largest flux recorded on these intervals.

Note that instead of the fluxes we employed their decimal logarithms for both the target variable and the features, namely electron fluxes in geostationary orbit. This is due to the fact that the fluxes have a wide dynamic range occupying several orders of magnitude.

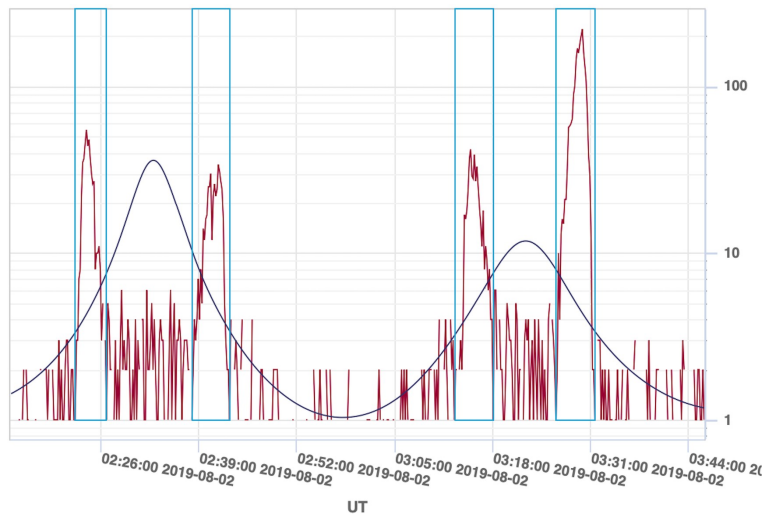


Figure 1. Electron fluxes in a circular polar orbit according to Meteor-M2 data (>0.7 MeV) and the McIlwain parameter L

3. INPUT DATA ANALYSIS

During the study, we have analyzed daily integral (Figures 2, 3) and maximum (Figures 4, 5) electron fluxes from Meteor-M2 and GOES data for >2 and >0.7 MeV (>0.8 MeV for GOES since there is no channel with the required energy threshold in the device). It has been found that there is a noticeable correlation between these fluxes, the moment of increase on both satellites coincides, whereas the decrease in the polar orbit is slower and smoother compared to the geostationary one.

In addition, we have analyzed daily average Dst , K_p , SW density and velocity, and IMF vector modulus (Figures 6–8). During the period considered, average Dst did not fall below -40 nT, which indicates the absence of strong geomagnetic storms during this period. However, the SW velocity periodically increased to 600–700 km/s with a period of ~ 26 days, which suggests the arrival of high-speed recurrent SW streams causing significant changes in near-Earth space and an increase in charged particle fluxes in radiation belts.

4. SELECTION OF INPUT FEATURES

The number of features obtained for the specified lookback window size is 126. This number may lead to

overfitting of linear regression on the time interval in use, so it is necessary to reduce the number of features. It is believed that the number of parameters in the machine learning model should be at least an order of magnitude smaller than the learning sample size [Alwosheel et al., 2018]. The corresponding calculation for our case (seven months, daily forecast) gives an estimate 10–20 for the maximum number of features.

The selection is based on the correlation coefficient of the feature considered with the target variable. The features with maximum (absolute) correlation are used for further forecasting.

The correlation coefficients for the integral electron flux with energies >2 and >0.7 MeV are shown in Figures 9 and 10 respectively. The maximum correlation of the >2 MeV integral electron flux is expected to be observed with the GOES integral flux, exceeding all others more than three times. This suggests that it is this flux which will make the main contribution to the forecast. The next most important are also expected to be the SW velocity, K_p , and Dst , which is consistent with existing concepts.

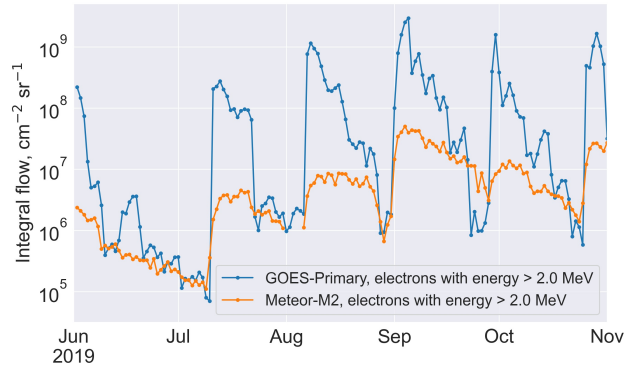


Figure 2. Total integral electron fluxes >2.0 MeV over the span of a day according to Meteor-M2 and GOES-Primary data

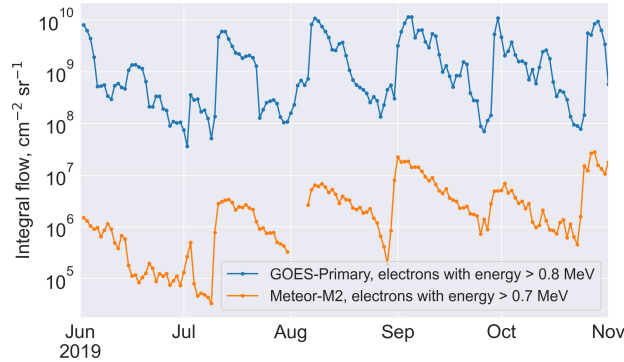


Figure 3. Total integral electron fluxes >0.7 and >0.8 MeV over the span of a day according to data from Meteor-M2 and GOES-Primary respectively

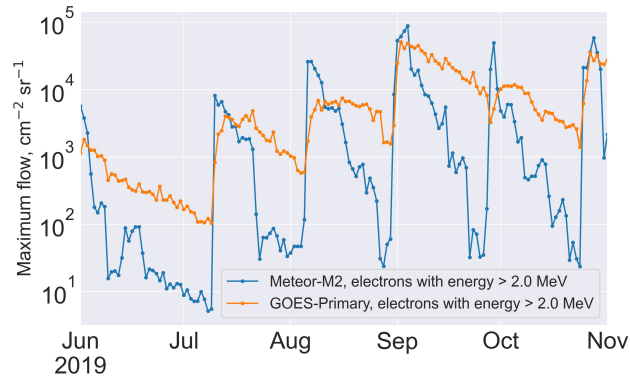


Figure 4. Daily maximum electron fluxes >2.0 MeV according to Meteor-M2 and GOES-Primary data

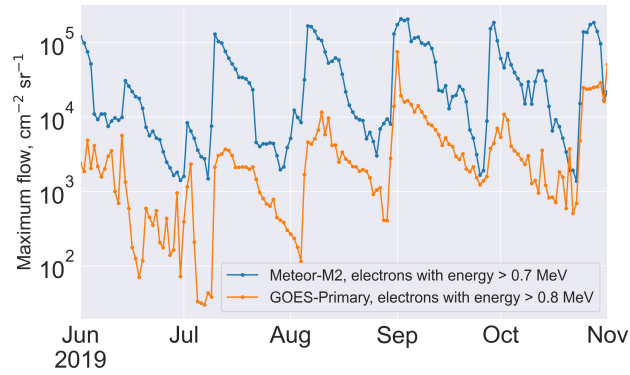


Figure 5. Daily maximum electron fluxes >0.7 and >0.8 MeV according to data from Meteor-M2 and GOES-Primary respectively

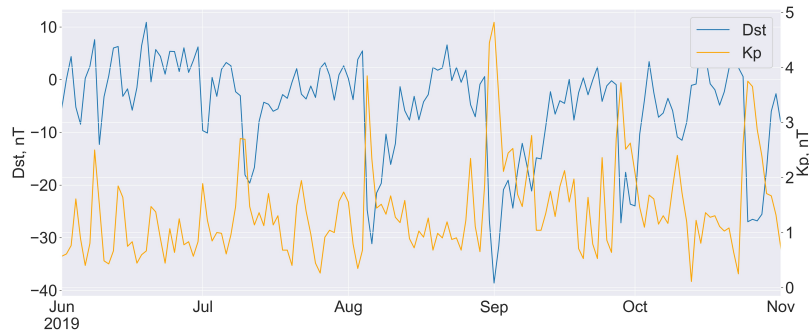


Figure 6. Daily average Dst and K_p

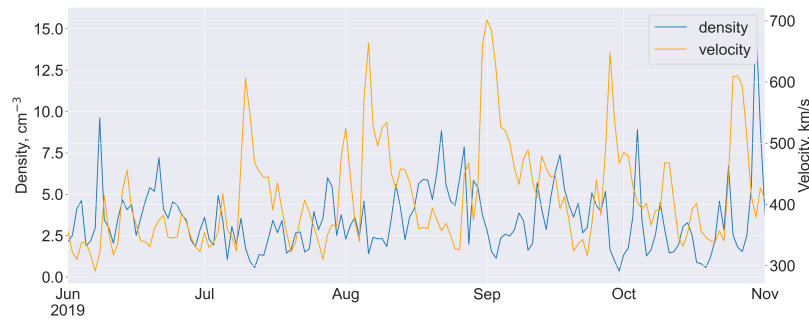
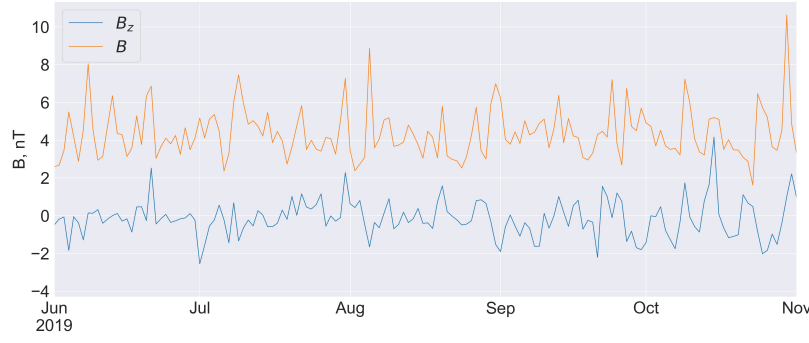
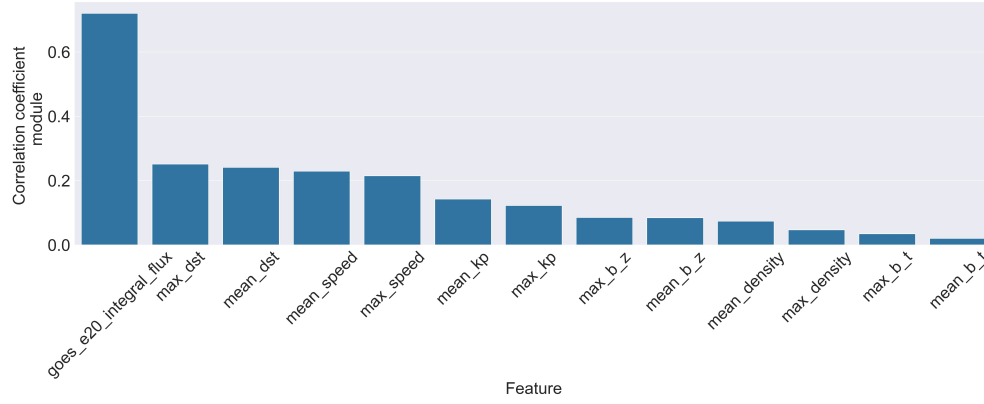
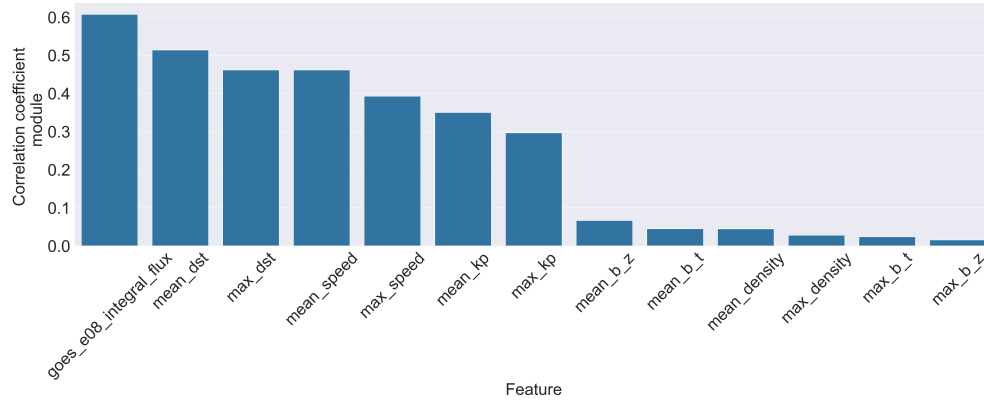


Figure 7. Daily average SW velocity and density


 Figure 8. Daily average B_z and B_t

 Figure 9. Modulus of the correlation coefficient of >2 MeV daily integral electron flux

 Figure 10. Modulus of the correlation coefficient of >0.7 MeV daily integral electron flux

For an energy of 0.7 MeV, the maximum correlation coefficient also belongs to the GOES integral flux, yet in this case it slightly exceeds the other coefficients, which indicates a higher variability in sub-relativistic electron fluxes compared to relativistic ones.

Note that the daily averages show a higher (absolute) correlation than the maximum values, which confirms the need to use them for forecasting.

5. FORECAST RESULTS

Daily forecasts for integral and maximum electron fluxes, made using linear regression and the naive model, are shown in Figures 11–18 (k is the number of features employed to make this forecast).

The results of prediction of >2 MeV electron fluxes appeared to be much better, which is probably due to their higher quasi-stationarity. Maximum fluxes are predicted less accurately than integral ones since they have a large spread of values over the span of several days.

To assess the quantitative measure of the forecast quality, we calculated the multiple determination coefficient R^2 and the root mean square error. The calculation was made with the test dataset, i.e. the data that was not used for training the model.

To analyze the quality of the model for solving this problem, we made a forecast with the aid of the naive model and calculated its characteristics. The values are presented in Table. The best indicators for each of the

forecast horizons and for a given energy are highlighted in blue. It can be seen that in all cases the naive forecast shows worse results than that made with linear regression. It has also been found that for $E > 0.7$ MeV the forecast of integral fluxes is better; and for $E > 2$ MeV, the forecast of

maximum fluxes. With an increase in the forecast horizon, a significant deterioration in the quality of forecasts for both energy ranges is expected.

Metrics of machine learning models
used in the problem of forecasting >0.7 and >2 MeV electron fluxes

	Forecast for 1 day		Forecast for 2 days	
Forecast of >0.7 MeV daily integral electron fluxes				
Model\Metrics	R^2	RMSE	R^2	RMSE
Naive forecast	0.663	0.325	0.382	0.439
Linear regression	0.696	0.308	0.550	0.375
Forecast of >0.7 MeV daily maximum electron fluxes				
Model\Metrics	R^2	RMSE	R^2	RMSE
Naive forecast	0.372	0.471	−0.046	0.608
Linear regression	0.558	0.395	0.316	0.492
Forecast of >2 MeV daily integral electron fluxes				
Model\Metrics	R^2	RMSE	R^2	RMSE
Naive forecast	0.819	0.156	0.603	0.232
Linear regression	0.825	0.154	0.708	0.199
Forecast of >2 MeV daily maximum electron fluxes				
Model\Metrics	R^2	RMSE	R^2	RMSE
Naive forecast	0.852	0.144	0.721	0.198
Linear regression	0.888	0.125	0.776	0.177

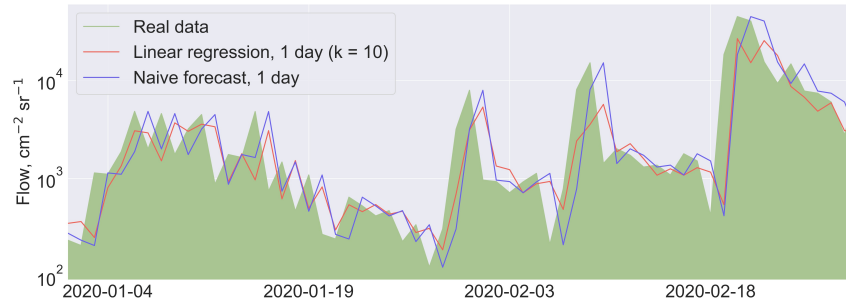


Figure 11. Forecast of >0.7 MeV daily maximum electron fluxes for 1 day

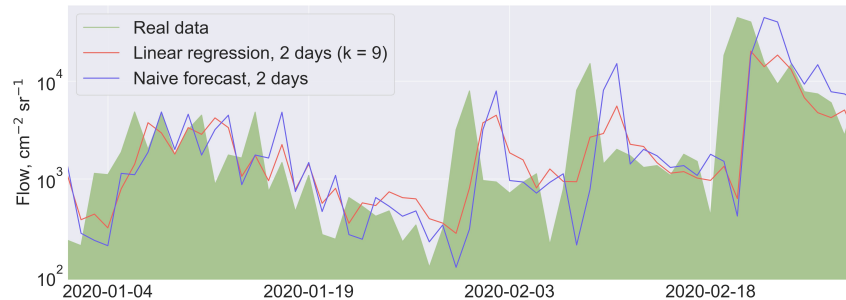


Figure 12. Forecast of >0.7 MeV daily maximum electron fluxes for 2 days

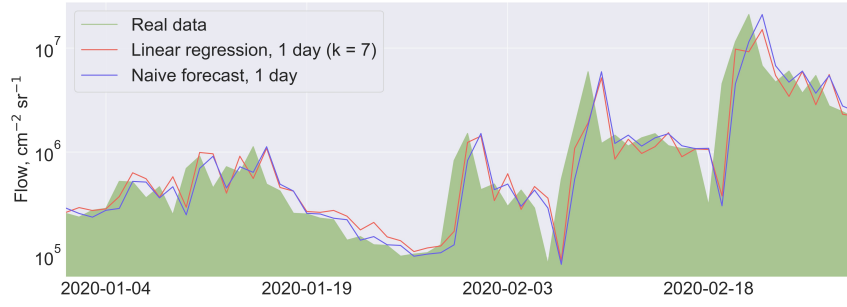


Figure 13. Forecast of >0.7 MeV daily integral electron fluxes for 1 day

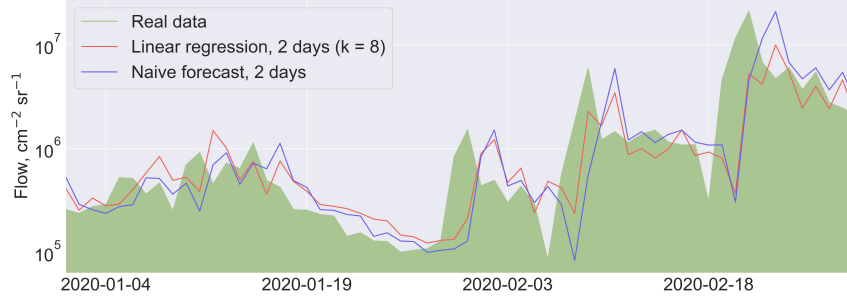


Figure 14. Forecast of >0.7 MeV daily integral electron fluxes for 2 days

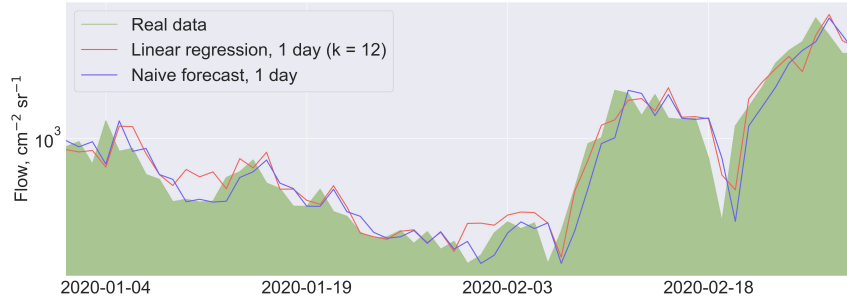


Figure 15. Forecast of >2 MeV daily maximum electron fluxes for 1 day

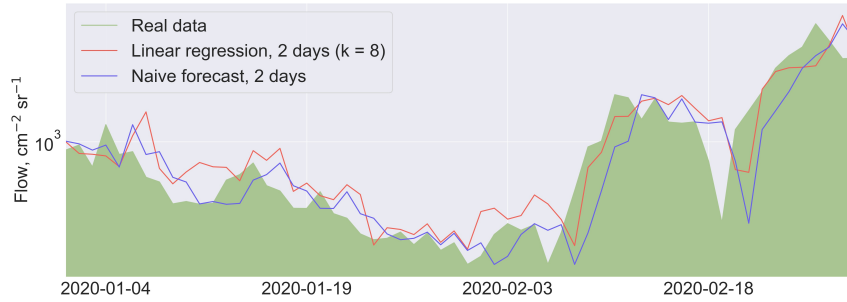


Figure 16. Forecast of >2 MeV daily maximum electron fluxes for 2 days

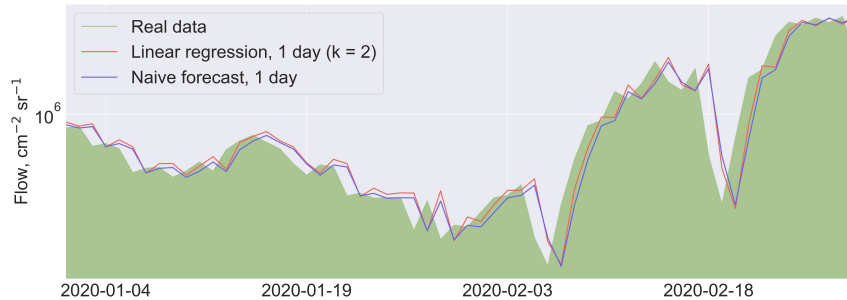


Figure 17. Forecast of >2 MeV daily integral electron fluxes for 1 day

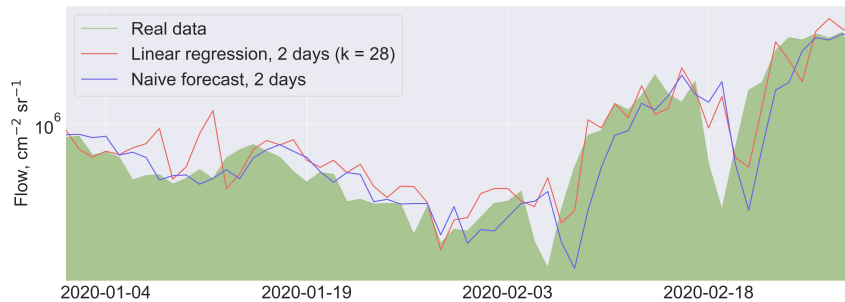


Figure 18. Forecast of >2 MeV daily integral electron fluxes for 2 days

CONCLUSION

The paper presents the results of the study of the possibility of predicting variations in >0.7 and >2 MeV electron fluxes (with the logarithm of flux) from Earth's outer radiation belt, measured in a circular polar orbit. The forecast was made using machine learning, where the solar wind and interplanetary magnetic field parameters, as well as geomagnetic indices and the logarithm of EORB electron flux in geostationary orbit were used as input features. We have selected optimal input features for predicting the electron flux in a low polar orbit. It has been found that in the polar orbit the maximum correlation of the >2 MeV integral electron flux in EORB is observed with the integral flux in geostationary orbit (GOES). In combination with the available results of prediction of electron fluxes in geostationary orbit for several days in advance [Myagkova et al., 2021; Kalegaev et al., 2023], the formulation of the problem of predicting electron fluxes in polar orbits can be considered promising.

From the results received during the study we can assume that in order to develop more accurate forecasting models the next possible step should be to expand the time series of experimental data in use, as well as to examine more complex machine learning models within this problem, such as artificial neural networks and gradient boosting.

The work was financially supported by the Russian Science Foundation (Grant No. 22-62-00048) [<https://rscf.ru/project/22-62-00048/>].

REFERENCES

- Alwosheel A., van Cranenburgh S., Chorus C.G. Is your dataset big enough? Sample size requirements when using artificial neural networks for discrete choice analysis. *J. Choice Modelling*. 2018, vol. 28, pp. 167–182. DOI: [10.1016/j.jocm.2018.07.002](https://doi.org/10.1016/j.jocm.2018.07.002).
- Baker D.N., McPherron R.L., Cayton T.E., Klebesadel R.W. Linear prediction filter analysis of relativistic electron properties at 6.6 RE. *J. Geophys. Res.* 1990, vol. 95, iss. A9, pp. 15133–15140. DOI: [10.1029/JA095iA09p15133](https://doi.org/10.1029/JA095iA09p15133).
- Belov A.V., Villaresi J., Dorman L.I., et al. The influence of the space environment on the functioning of artificial Earth satellites. *Geomagnetism and Aeronomy*. 2004, vol. 44, iss. 4, pp. 502–510.
- Balikhin M.A., Boynton R.J., Walker S.N., et al. Using the NARMAX approach to model the evolution of energetic electrons fluxes at geostationary orbit. *Geophys. Res. Lett.* 2011, vol. 38, iss. 18. DOI: [10.1029/2011GL048980](https://doi.org/10.1029/2011GL048980).
- Botek E., Pierrard V., Winant A. Prediction of radiation belts electron fluxes at a Low Earth Orbit using neural networks with PROBA-V/EPT data. *Space Weather*. 2023, vol. 21, iss. 7, e2023SW003466. DOI: [10.1029/2023SW003466](https://doi.org/10.1029/2023SW003466).
- Cole D.G. Space weather: Its effects and predictability. *Space Sci. Rev.* 2003, vol. 107, pp. 295–302. DOI: [10.1023/A:1025500513499](https://doi.org/10.1023/A:1025500513499).
- Demidenko E.Z. *Linear and nonlinear regression*. Moscow: Finance and Statistics, 1981, 302 p.
- Denton M.H., Henderson M.G., Jordanova V.K., et al. An improved empirical model of electron and ion fluxes at geosynchronous orbit based on upstream solar wind conditions. *Space Weather*. 2016, vol. 14, iss. 7, pp. 511–523. DOI: [10.1002/2016SW001409](https://doi.org/10.1002/2016SW001409).
- Glauert S.A., Horne R.B., Meredith N.P. Three-dimensional electron radiation belt simulations using the BAS Radiation Belt Model with new diffusion models for chorus, plasmaspheric hiss, and lightning-generated whistlers. *J. Geophys. Res.: Space Phys.* 2014, vol. 119, iss. 1, pp. 268–289. DOI: [10.1002/2013JA019281](https://doi.org/10.1002/2013JA019281).
- Iucci N., Levitin A., Belov E., et al. Space weather conditions and spacecraft anomalies in different orbits. *Space Weather*. 2005, vol. 3, iss. 1. DOI: [10.1029/2003SW000056](https://doi.org/10.1029/2003SW000056).
- Kalegaev V., Panasyuk M., Myagkova I., et al. Monitoring, analysis and post-casting of the Earth's particle radiation environment during February 14 – March 5, 2014. *Space Weather Space Climate*. 2019, vol. 9, iss. A29. DOI: [10.1051/swsc/2019029](https://doi.org/10.1051/swsc/2019029).
- Kalegaev V., Kaportseva K., Myagkova I., et al. Medium-term prediction of the fluence of relativistic electrons in geostationary orbit using solar wind streams forecast based on solar observations. *Adv. Space Res.* 2023, vol. 72, iss. 12, pp. 5376–5390. DOI: [10.1016/j.asr.2022.08.033](https://doi.org/10.1016/j.asr.2022.08.033).
- Kataoka R., Miyoshi Y. Average profiles of the solar wind and outer radiation belt during the extreme flux enhancement of relativistic electrons at geosynchronous orbit. *Ann. Geophys.* 2008, vol. 26, iss. 6, pp. 1335–1339. DOI: [10.5194/angeo-26-1335-2008](https://doi.org/10.5194/angeo-26-1335-2008).
- Koons H.C., Gorney D.J. A neural network model of the relativistic electron flux at geosynchronous orbit. *J. Geophys. Res.* 1991, vol. 96, iss. A4, pp. 5549–5556. DOI: [10.1029/90JA02380](https://doi.org/10.1029/90JA02380).
- Kudela K. Space weather near Earth and energetic particles: Selected results. *J. Physics Conf. Ser.* 2013, vol. 409, iss. 1. DOI: [10.1088/1742-6596/409/1/012017](https://doi.org/10.1088/1742-6596/409/1/012017).
- Kuznetsov S.N., Myagkova I.N., Yushkov B.Yu., et al. Dynamics of the Earth's radiation belts during strong magnetic storms according to data from the CORONAS-F satellite. *Astronomical Bulletin. Studies of the Solar System*. 2007, vol. 41, iss. 4, pp. 369–378.
- Landis D.A., Saikin A.A., Zhelavskaya I., et al. NARX neural network derivations of the outer boundary radiation belt

- electron flux. *Space Weather*. 2022, vol. 20, iss. 5, e2021SW002774. DOI: [10.1029/2021SW002774](https://doi.org/10.1029/2021SW002774).
- Li W., Hudson M.K. Earth's Van Allen radiation belts: From discovery to the Van Allen Probes era. *J. Geophys. Res.: Space Phys.* 2019, vol. 124, iss. 11, pp. 8319–8351. DOI: [10.1029/2018JA025940](https://doi.org/10.1029/2018JA025940).
- Li X., Baker D.N., Kanekal S.G., et al. Long term measurements of radiation belts by SAMPEX and their variations. *Geophys. Res. Lett.* 2001, vol. 28, iss. 20, pp. 3827–3830. DOI: [10.1029/2001gl013586](https://doi.org/10.1029/2001gl013586).
- Ling A.G., Ginot G.P., Hilmer R.V., Perry K.L. A neural network-based geosynchronous relativistic electron flux forecasting model. *Space Weather*. 2010, vol. 8, iss. 9. DOI: [10.1029/2010SW000576](https://doi.org/10.1029/2010SW000576).
- Lyatsky W., Khazanov G.V. A predictive model for relativistic electrons at geostationary orbit. *Geophys. Res. Lett.* 2008, vol. 35, iss. 15, L15108. DOI: [10.1029/2008GL034688](https://doi.org/10.1029/2008GL034688).
- Myagkova I., Efitorov A., Shiroky V., Dolenko S.A. Quality of prediction of daily relativistic electrons flux at geostationary orbit by machine learning methods. *Artificial Neural Networks and Machine Learning – ICANN 2019: Text and Time Series*. 2019, pp. 556–565. DOI: [10.1007/978-3-030-30490-4_45](https://doi.org/10.1007/978-3-030-30490-4_45).
- Myagkova I.N., Shirokiy V.R., Shugai Yu.S., et al. Short- and medium-term forecasting of relativistic electron fluxes in the Earth's outer radiation belt using machine learning methods. *Meteorology and Hydrology*. 2021, iss. 3, pp. 47–57. DOI: [10.52002/0130-2906-2021-3-47-57](https://doi.org/10.52002/0130-2906-2021-3-47-57).
- Novikov L.S., Voronina E.N. *Interaction of Spacecraft with the Environment*. Moscow: KDU, 2021, 560 p.
- Osedlo V.I., Kalegaev V.V., Rubinshtein I.A., et al. Monitoring the radiation state of the near-Earth space on the Arktika-M No. 1 Satellite. *Cosmic Res.* 2022, vol. 60, iss. 6, pp. 406–419. DOI: [1134/S0010952522060089](https://doi.org/10.1134/S0010952522060089).
- Pilipenko V., Yagova N., Romanova N., Allen J. Statistical relationships between the satellite anomalies at geostationary orbits and high-energy particles. *Adv. Space Res.* 2006, vol. 37, iss. 6, pp. 1192–1205. DOI: [10.1016/j.asr.2005.03.152](https://doi.org/10.1016/j.asr.2005.03.152).
- Potapov A., Ryzhakova L., Tsegmed B. A new approach to predict and estimate enhancements of "killer" electron flux at geosynchronous orbit. *Acta Astronaut.* 2016, vol. 126, pp. 47–51. DOI: [10.1016/j.actaastro.2016.04.017](https://doi.org/10.1016/j.actaastro.2016.04.017).
- Romanova N.V., Pilipenko V.A., Yadova N.V., Belov A.V. Statistical relationship of the frequency of failures on geostationary satellites with the fluxes of energetic electrons and protons. *Space Res.* 2005, vol. 43, iss. 3, pp. 186–193.
- Son J., Moon Y.-J., Shin S. 72-hour time series forecasting of hourly relativistic electron fluxes at geostationary orbit by deep learning. *Space Weather*. 2022, vol. 20, iss. 10, e2022SW003153. DOI: [10.1029/2022sw003153](https://doi.org/10.1029/2022sw003153).
- Stepanova M., Pinto V., Antonova E. Regarding the relativistic electron dynamics in the outer radiation belt: a historical view. *Rev. Modern Plasma Physics*. 2024, vol. 8, iss. 25. DOI: [10.1007/s41614-024-00165-4](https://doi.org/10.1007/s41614-024-00165-4).
- Sun X., Lin R., Liu S., et al. Modeling the relationship of ≥ 2 MeV electron fluxes at different longitudes in geostationary orbit by the machine learning method. *Remote Sensing*. 2021, vol. 13, iss. 17, p. 3347. DOI: [10.3390/rs13173347](https://doi.org/10.3390/rs13173347).
- Vernov S.N., Grigorov N.L., Logachev Yu.I., Chudakov A.E. Measurements of cosmic radiation on an artificial Earth satellite. *Reports of the Academy of Sciences*. 1958, vol. 120, iss. 6, pp. 1231–1233.
- Wei L., Zhong Q., Lin R., et al. Quantitative prediction of high-energy electron integral flux at geostationary orbit based on deep learning. *Space Weather*. 2018, vol. 16, iss. 7, pp. 903–916. DOI: [10.1029/2018SW001829](https://doi.org/10.1029/2018SW001829).
- Williams D.J., Arens J.F., Lanzerotti L.J. Observations of trapped electrons at low and high altitudes. *J. Geophys. Res.* 1968, vol. 73, iss. 17, pp. 5673–5696. DOI: [10.1029/ja073i017p05673](https://doi.org/10.1029/ja073i017p05673).

The paper is based on material presented at the 20th Annual Conference on Plasma Physics in the Solar System, February 10–14, 2025, Space Research Institute of the Russian Academy of Sciences, Moscow, Russia.

Original Russian version: Gololobov P.Yu., Grigoryev V.G., Gerasimova S.K., published in *Solnechno-zemnaya fizika*. 2025, vol. 11, no. 3, pp. 77–87. DOI: [10.12737/szf-113202509](https://doi.org/10.12737/szf-113202509). © 2025 INFRA-M Academic Publishing House (Nauchno-Izdatelskii Tsentr INFRA-M).

How to cite this article

Belova A.O., Myagkova I.N. Prediction of electron fluxes in a circular polar orbit: Selection of predictors. *Sol.-Terr. Phys.* 2025, vol. 11, iss. 3, pp. 70–79. DOI: [10.12737/stp-113202509](https://doi.org/10.12737/stp-113202509).